The 3rd International Conference on Civil Engineering Innovations & Advancements (ICCEIA 2026)
August 20–22, 2026 – London, United Kingdom
Paper No. ICCEIA 003
DOI: 10.11159/icceia26.003

# From Innovation to Implementation: SMA-Augmented Tension Rods for Resilient Design at the Grimes Engineering Center

**Rupa Garai[1], David Shook[1], Shakhzod Takhirov[2], Amarnath Kasalanati[3], Selim Günay[3], Khalid M. Mosalam[2,3,*]**

[1]Skidmore, Owings & Merrill (SOM)
One Maritime Plaza, San Francisco, CA 94111, USA
rupa.garai@som.com; david.shook@som.com

[2]Department of Civil & Environmental Engineering (CEE)
[3]Pacific Earthquake Engineering Research (PEER) Center
Davis Hall, University of California, Berkeley, CA 94720-1710, USA
takhirov@berkeley.edu; amarnath1@berkeley.edu; selimgunay@berkeley.edu;
mosalam@berkeley.edu

[*]*Corresponding Author & Presenter*

***Abstract –*** This paper presents the design, implementation, and validation of shape memory alloy (SMA)-augmented tension rods for seismic response mitigation at the University of California, Berkeley's Grimes Engineering Center (GEC). The SMA devices, integrated with buckling-restrained braces (BRBs), reduce torsional response, floor accelerations, peak and residual drifts, and demands on structural members, thereby enhancing post-earthquake functionality.

The system was validated through multi-scale experimental testing, including component, device, and frame-level tests, as well as in-situ field measurements. Results demonstrate stable hysteretic behavior, strong self-centering capability, and good agreement between measured and predicted responses. The study highlights the feasibility of implementing SMA-based recentering systems in building-scale applications.

**Keywords:** buckling-restrained braces, field verification, seismic resilience, shape memory alloy, structural testing, tension rods

## 1. Introduction

The application of innovative materials, components, and systems to improve seismic performance in practical applications requires a thoughtful and rigorous research investigation that includes material testing, component testing, numerical modeling, practical detailing, defined operational ranges, and reliable failure mechanisms. When possible, both static and dynamic testing can be pursued to gain a more complete understanding of potential behaviors. Shape-memory alloy (SMA) are among such innovative materials.

SMA is a metallic material composed of two or more elements that, when alloyed and heat-treated, exhibit a reversible solid-state phase transformation that allows them to recover a predefined shape after deformation. Depending on composition and heat treatment, SMA can exhibit two distinct behaviors: superelasticity and the shape memory effect.

- **Superelastic effect:** A strain-induced, solid-state phase transformation that enables large, fully recoverable strains, even under significant deformation (e.g., up to approximately 6% in Nitinol).
- **Shape memory effect:** A thermally induced, solid-state phase transformation by which an SMA recovers a previously defined geometry after being deformed.

For this application, superelastic Nitinol, a nickel–titanium shape memory alloy, is used. It can sustain recoverable strains of approximately 6%, significantly exceeding conventional structural steel ($\approx 0.2\%$). This behavior enables efficient energy dissipation and recentering, making SMA particularly suitable for seismic applications. Further details on SMA behavior and applications are available in the literature, e.g., [1–4].

This study focuses on the use of SMAs to increase the post-earthquake resilience and rapid reoccupancy capability of a major campus building at the University of California, Berkeley (UCB), namely the Grimes

Engineering Center (GEC). The paper presents the experimental studies, field verification, and numerical simulations that support the design and implementation of this system.

## 2. Project Context

The GEC at UCB is a seismic renovation and addition to the Bechtel Engineering Center. The building site is only a quarter mile from the north–south-trending Hayward Fault, which has a 33% probability of producing a magnitude 6.7 or larger earthquake before 2043. Therefore, seismic performance was the major consideration in the renovation and addition design.

The original Bechtel Engineering Center had extensive landscaping on its roof, consisting of a thick gravel drainage layer, a topping slab, and 1′ to 3′ of soil. The new building removed this landscape, and the weight of the new floors is approximately equal to that of the existing landscaping. This minimized the retrofit work on the existing reinforced concrete structure.

The new building was designed in accordance with the California Building Code and the UCB Campus Design Standards, including the UC Berkeley Seismic Guidelines and an ASCE 41 Tier 3 evaluation [5]. In the building numerical model, the following components used nonlinear modeling: shear and flexure in existing shear walls, rotation at new steel beam ends, rotation at new steel columns' ends, SMA cables, axial tension yielding and compression buckling of the tension rod, tension/compression of buckling-restrained braces (BRBs), and compression-only soil springs under footings supporting columns below the BRB frames. While modal response spectrum analysis was used for early proportioning, the lateral–force–resisting system design, including BRBs and SMA tension rods, was conducted using nonlinear response-history analysis.

The steel columns are HSS $12 \times 12$ sections; the framing at Level 2 terrace and Level 3 consists of W21 girders and W18 joists; and the roof framing consists of double MC18 members along gridlines and W14 joists between them. BRB frames utilize wide-flange beams with a single-pin connection to gusset plates. The existing pan-joist system typically consists of a 4.5-in one-way slab supported by 20-in joists, resulting in a total depth of 24.5″. Fiber reinforced polymers (FRP) was applied to the diaphragm and to a few beams. Only a few footings under the BRBs required retrofit because of increased loads. All new columns are placed on existing columns. Fig. 1(a) is a rendering illustrating the existing and new construction of the building.

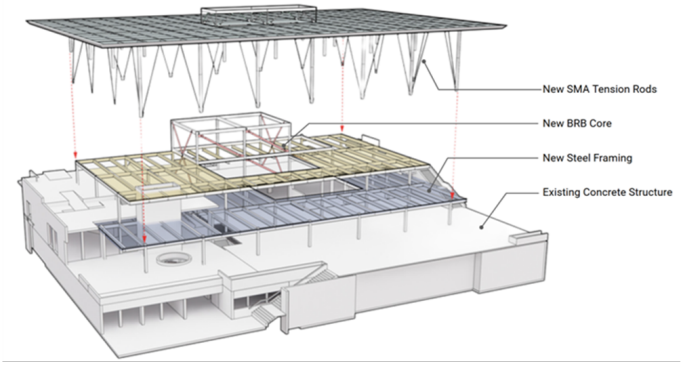


(a) Existing and new construction.

(b) Completed building.

Fig. 1: Grimes Engineering Center.

The center of the building includes a large "forum" space, a common area for students and faculty to use for a broad range of functions. The BRB core would need to be shifted to maximize the openness and function of the forum. Therefore, the BRB core was shifted eccentrically relative to the new building, resulting in a primarily torsional response (particularly in the east-west direction) when subjected to ground motions. To mitigate this response, a light perimeter system was envisioned, integrated with the architectural design, to efficiently reduce torsion while avoiding heavy demands on existing concrete columns and footings.

A tension rod system at the perimeter is desirable to mitigate torsion, except for the tension rod's poor performance in strong ground motions, where axial elongation results in unpredictable response. Skidmore, Owings & Merrill (SOM) engineers considered a range of options, including small viscous dampers, friction-based devices, and SMA cables to insert a "fuse" in the tension rod, thereby protecting the tension rod and mitigating unreliable behavior while introducing additional damping. The fuse candidates were evaluated considering cost, performance, and potential repair and maintenance. Based on collaboration with university representatives, peer review panels, and cost estimates, SMA tension rods were selected for incorporation.

With the structural system otherwise unchanged, the inclusion of SMA tension rods reduced floor accelerations, peak story drifts, and torsional response (due to uniform stiffness contribution of perimeter SMA frames and SMA modal damping) by about 10%, 20%, and 35%, respectively, reduced residual story drifts by 50% on average (with some reductions as high as 75%) mainly due to reduction in torsional response, and reduced BRB frame demands. Although the building was not explicitly designed for functional recovery, these improvements are expected to facilitate post-earthquake reoccupancy. If the building had been designed without SMA, the BRB sizes would likely have been increased and/or additional BRBs would have been added in the north-south (the concentric) direction to control torsion. This would have increased the column and beam sizes in the BRB frame and affected the supporting reinforced concrete columns and footings below. Fig. 1(b) illustrates the completed building.

## 3. Proof-of-Concept Shaking Table Testing

After SMA was selected as the fuse element in the tension-rod system, the next step was to finalize the detailing of the SMA tension rods. Initially, SOM selected Nitinol as the superelastic SMA for this application because it is available as a cable from vendors in a range of wire diameters and cable configurations. Additionally, Nitinol's stable hysteresis across typical temperature ranges, resistance to corrosion, and low strain-rate dependence [2] provided an opportunity to use superelastic SMA in a new building in a high-seismic region. The SMA material can be difficult to attach using conventional methods such as welding, bolting, or threading. A novel approach proposed in prior work used individual SMA wires assembled into a rope and connected to carbon steel by swaging a threaded bolt to the end of the SMA cable. The reported results indicated that the *swage connection* can fully develop the strength of the SMA cable and ensure failure away from the bolt for a reliable and ductile connection up to ultimate strength. SOM obtained two cable sizes and swage anchors from multiple vendors to evaluate and confirm that the favorable behavior observed in the literature could be reliably repeated across a range of cable sizes, swage bolt types, and vendors. Based on this testing, a reliable SMA cable vendor was selected and the swage anchor type was confirmed. With material and swage connections confirmed, SOM then conducted large-scale dynamic testing at the Pacific Earthquake Engineering Research Center (PEER) six-degrees-of-freedom 20 ft × 20 ft shaking table. Testing was conducted using PEER's three-story modular steel frame, known as the REconfigurable Platform for EArthquake Testing (REPEAT) frame.

The three-story frame was initially tested without any SMA tension rods to determine its fundamental period and estimate damping. The fundamental periods were identified from white noise tests. The damping ratios were identified by exciting the structure in each of the three modes of vibration for a few cycles and recording the consequent free vibrations. The first three periods were identified as 0.50 s (representative of buildings similar to the GEC), 0.14 s, and 0.04 s. The first-mode damping ratio was approximately 3% (representative of steel buildings without SMA rods). The SMA tension rods were fabricated off-site and shipped to the laboratory. The team assembled the tension rods, installed transducers, and applied a modest pre-stressing to the tension rods. Instrumentation included displacement, acceleration, and force measurements to capture component and system response (see Fig. 2).

A suite of ground motions with increasing intensity (25% to 100%) was applied. During the most demanding motions, the SMA cables experienced tensile strains of approximately 6%. The stresses discussed below were measured using load cells attached to the tension rods. Dynamic interaction effects were observed

Fig. 2: Preparing instrumentation for the shaking table testing.

due to the inertia of the tension rods, including transient force fluctuations and out-of-plane (OOP) motion. This led to the incorporation of a center rod in the final design. Other key observations include the following:

- SMA cables experienced neither failure nor permanent deformation during the shaking table tests.
- SMA swage anchors and the tension rod assembly remained intact with no signs of slippage or failure.
- The SMA tension rod system performed consistently across multiple, repeated high-magnitude ground motions without any repair, adjustment, or tightening.
- The frame experienced slight stiffening due to the tension in the SMA devices. This was determined based on system identification of the free vibration response with and without the SMA tension rods.

The blind prediction results using an ETABS [6] model, conducted before the tests, and their comparisons to the experimental measurements are shown in Fig. 3. These results are for two shaking table runs (50% and 75% scales) of ground motions from the magnitude 7.6 Chi-Chi earthquake, which occurred in Taiwan in 1999. It was observed that the inertial demands of the tension rod moving out of centerline affected the recorded tension and compression forces. The inertial mass of the tension rod was included in the analysis, but the out-of-centerline movement of the tension rod was not included because of software limitations. The maximum recorded strain and stress were 3.3% and 70 ksi at the 50% scale level. At the 75% scale level, these values increased to 4.4% ($\approx$ 33% increase) and 83 ksi ($\approx$ 19% increase), respectively.

## 4. Project Validation Quasi-Static Testing

The shaking table tests conducted in the earthquake simulation laboratory at PEER, which used scaled SMA tension rods, discussed in the previous section, served as initial proof-of-concept tests. These tests

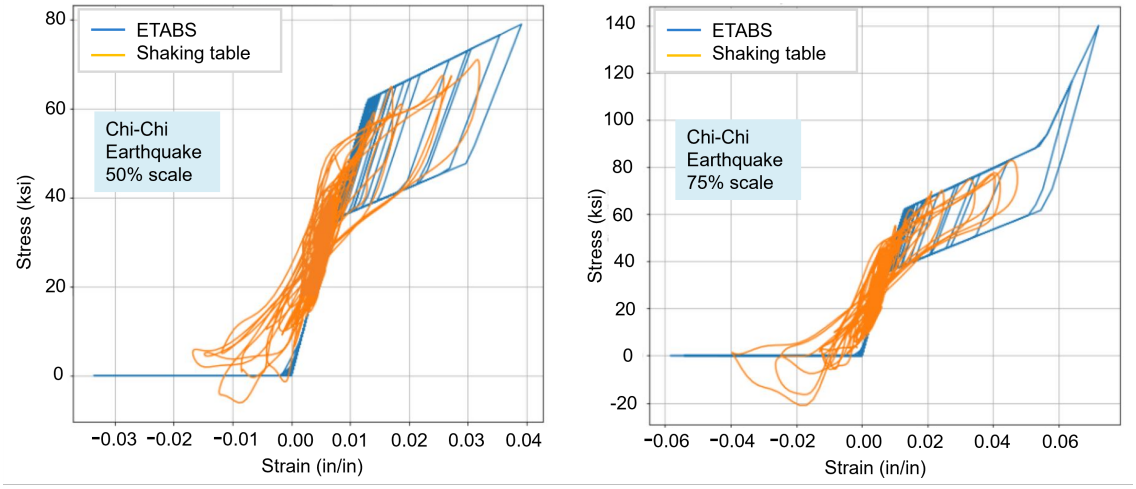


Fig. 3: Example blind prediction (using an ETABS [6] computer model developed by SOM engineers) and measured tension rod force from the shaking table tests.

were followed by another set of experimental studies that consisted of two major phases. The first phase was full-scale component testing under quasi-static loading to validate the performance of the SMA cables and devices under cyclic loading and to investigate the governing failure modes. The second phase focused on frame-level testing of scaled-down SMA devices in a representative perimeter frame in the actual building. The quasi-static cyclic and failure tests were conducted at the structures laboratory of the Department of Civil and Environmental Engineering (CEE) at UCB.

### 4.1. Full-scale SMA cable tests

Individual SMA cables were tested under quasi-static loading to failure (see Fig. 4(a)). Subjecting the SMA cable to controlled cyclic loading and/or thermal cycles before installation (pre-training) was essential to achieve stable hysteretic response. The results in Fig. 4(b) showed consistent superelastic behavior, with ultimate strains exceeding 14% and minor variability between specimens (cables 1 & 2 were pre-trained and not pre-trained, respectively). After heat treatment, superelastic SMA must undergo about 10 to 30 cycles for the lattice to undergo its phase changes. The Nitinol cables are highly consistent after training has occurred.

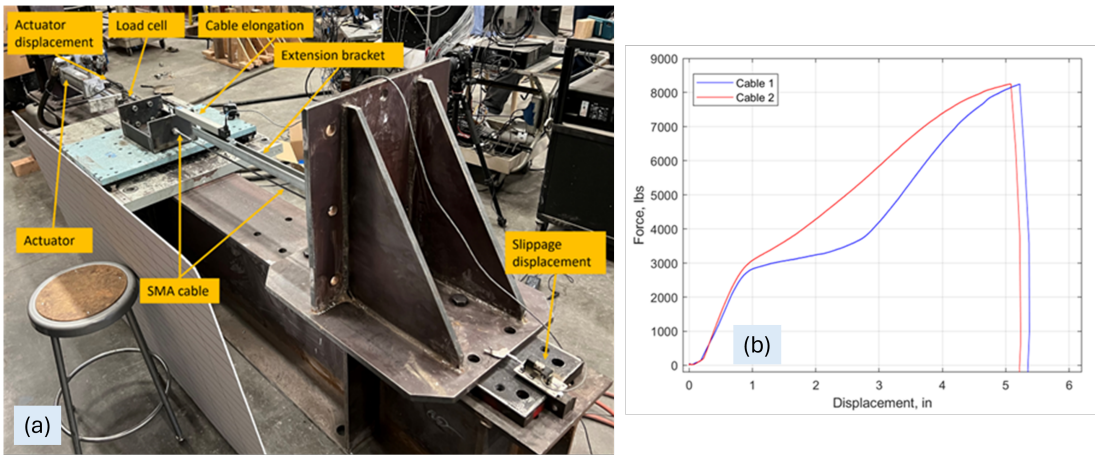


Fig. 4: Experimental setup for individual SMA cable testing (a) and quasi-static pull-to-failure results for two individual SMA cables, 1 & 2 (b).

### 4.2. Full-scale SMA device tests

Full-scale SMA devices were tested under cyclic and monotonic loading; Fig. 5(a) shows the test setup. Two devices were used to evaluate cyclic behavior, with the first one later subjected to repeated low-amplitude cycles followed by monotonic tension to failure. For brevity, those results are omitted here. The second full-scale device, SMA-FS-03, was tested under cyclic loading with additional groups of increasing displacement amplitude, and its response is shown in Fig. 5(b). The results demonstrated stable hysteretic behavior, strong recentering capability, and a tensile capacity of approximately 150 kips, consistent with the cable tests.

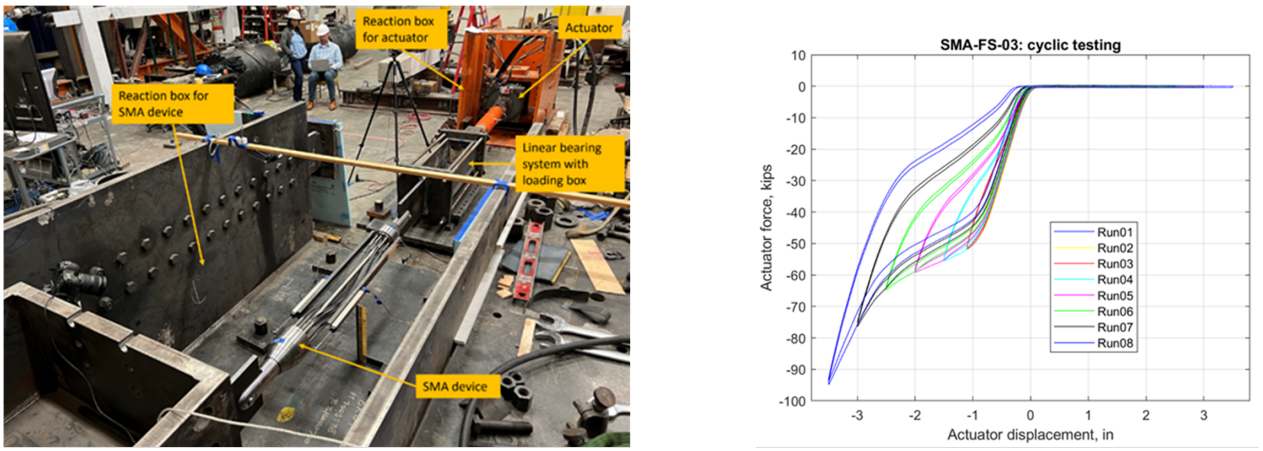


(a) (b)

Fig. 5: SMA device evaluation: (a) full-scale experimental setup; (b) force–displacement response of specimen SMA-FS-03.

### 4.3. Reduced-scale SMA-braced frame tests

A reduced-scale (1/6) frame test was conducted to evaluate system-level performance. To explore the response of this reduced-scale specimen, a special experimental setup was developed at the CEE structures laboratory. Fig. 6(a) illustrates the details of this setup. A special gravity-load system that used lead blocks was developed to apply the specified dead load of approximately 5.7 kips on each column. The gravity load was suspended from a $5'' \times 5''$ HSS welded on top of the beam at each column. Fig. 6(b) illustrates the details of this gravity-load system.

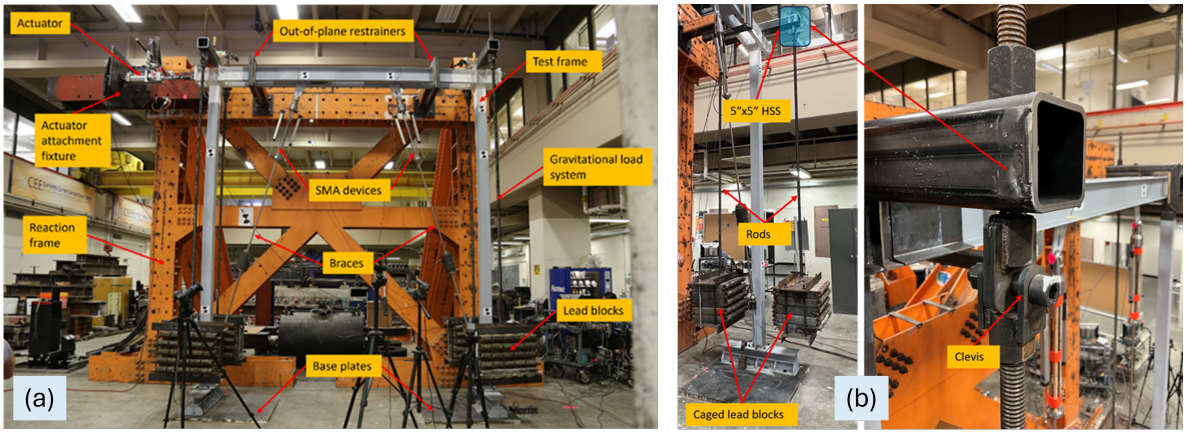


Fig. 6: Experimental setup for reduced-scale frame testing (a), and its gravity-load system (b).

A few low-level tests were conducted to check the instrumentation and hydraulic control. After completion of the low-level cycle tests, the main cyclic loading protocol with incrementally increasing displacement amplitude was imposed on the test frame, as shown in Fig. 7(a). The global lateral force–displacement relationship shown in Fig. 7(b) shows that the SMA-braced frame combined strong self-centering capability with appreciable energy dissipation. The obtained deformation history and the corresponding hysteresis loops of the SMA devices in this reduced-scale frame were analogous to those obtained in the full-scale SMA device tests (Section 4.2), i.e., clearly demonstrating the stability and repeatability of the SMA device response. The SMA deformation and force time histories, and the force–displacement relationships were also consistent between the two braces (N & S), demonstrating highly repeatable behavior.

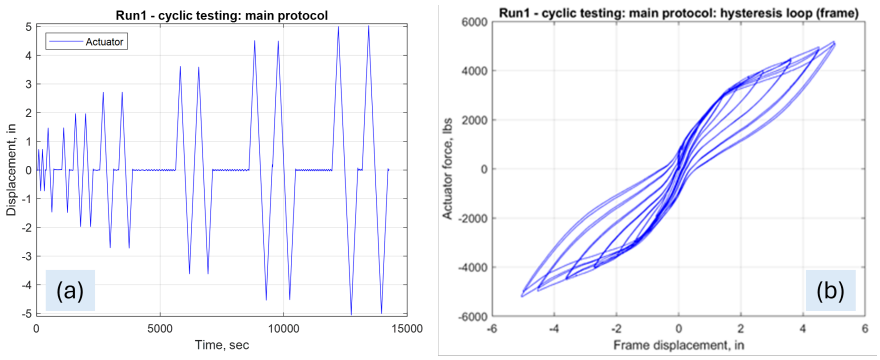


Fig. 7: Cyclic testing protocol with incrementally increasing displacement amplitudes (a), and lateral force–displacement relationship (b) of the tested reduced-scale SMA-braced frame.

## 5. Field Verification

Forced-vibration tests were conducted in February 2026 (ten months after the completion of the GEC) using an eccentric mass shaker (EMS, see Fig. 8(a)) to identify building modal properties in the NS, EW, and torsional directions. These tests were conducted during the regular operation of the building under ambient conditions. Vibration data were collected using PEER-CENTS (Cost-Effective Next Technology Sensor), a six-degree-of-freedom in-house sensor developed by PEER. This sensor can measure accelerations in three translational directions and rotational velocities about these three directions.

The EMS was situated on the second floor. In forced-vibration tests, an EMS is commonly placed at the roof level to generate the maximum possible vibrations. In these tests, however, the EMS was placed on the second floor because it was not possible to place it on the roof or on the third floor due to transportation and placement logistics. The EMS was connected to the base of an interior column (see Fig. 8) through steel rods to transfer the dynamic force excitation to the building. Measurements were obtained using PEER-CENTS sensors and conventional accelerometers at multiple floor levels (see Figs. 9 and 10).

The EMS was placed in two configurations to excite the modes in the NS, EW, and torsional directions. Because the first-mode frequencies ($f_n = 1/T_n$) were estimated to lie between 1.0 and 2.0 Hz, eleven forcing frequencies ($\omega = 2\pi f$ in Fig. 8) were applied between 0.6 Hz and 2.6 Hz in increments of 0.2 Hz. The excitation duration for each application was approximately 30 s followed by free vibration. The tests were conducted at different force–excitation levels with masses ($m_s$ in Fig. 8) varying between the basket weight only (106 lb/g) and several triangular and rectangular blocks placed in the baskets (634 lb/g).

Using the collected data, the dominant periods in the NS, EW, and torsional directions were identified as peaks of the transfer functions obtained by dividing the Fourier amplitude spectra of the response accelerations (measured by PC3) by those of the EMS accelerations (measured by PC1). The results are shown in Fig. 11. The PC3 rotational velocities measured about the vertical axis were used to develop the transfer function for the torsional mode. The identified fundamental periods in the NS, EW, and torsional directions were

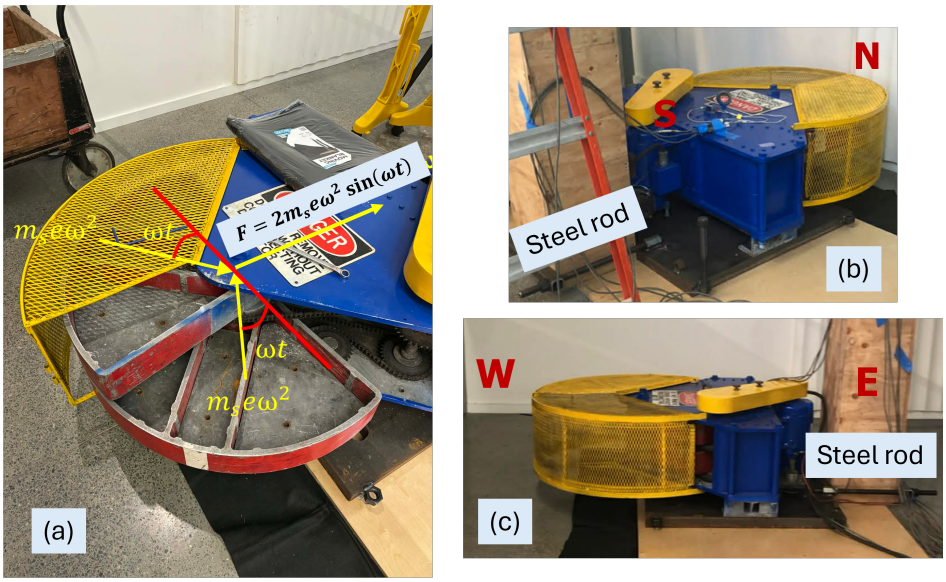


Fig. 8: Resultant-force generation of the EMS and its two field configurations, (a) The centripetal and resultant forces generated by the EMS, and (b, c) EMS placed along the EW and NS directions. Steel rods used to attach the EMS to the column are also visible.

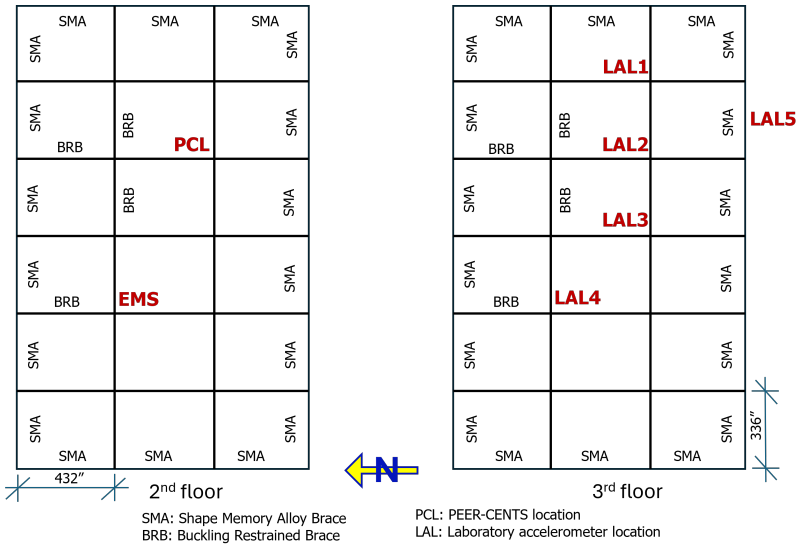


Fig. 9: Plan views of the 2nd and 3rd floors showing the EMS, PEER-CENTS (PCL at different locations vertically, see Fig. 10 for these locations), and the laboratory accelerometer locations (LAL1 to LAL5).

0.65 s, 0.78 s, and 0.85 s, respectively, which are in reasonable agreement with the corresponding periods obtained from the eigenvalue analysis of the numerical model of the building, namely 0.55 s, 0.67 s, and 0.88 s. Peaks close to the PEER-CENTS-identified periods of 0.65, 0.78, and 0.85 s also appeared in the transfer functions obtained using the conventional laboratory accelerometers. This supports both the use of PEER-CENTS in ambient vibration conditions for structural health monitoring (SHM) and the general accuracy of the developed numerical model. It is noted that the transfer functions from the conventional laboratory accelerometers were constructed using LAL3 in the NS and EW directions and the differential response between LAL3 and LAL2 in the torsional direction (Fig. 9), together with the EMS accelerations.

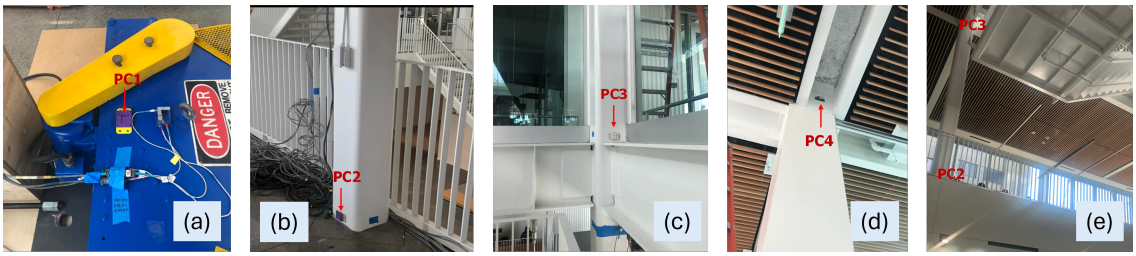


Fig. 10: PEER-CENTS installed on the EMS and at selected floor levels, (a) placed on the EMS, (b, c, d) attached to the column PCL (see Fig. 9) at the 2nd and 3rd floor levels and the roof directly mounted on the floor, and (e) attached to the column at the floor levels.

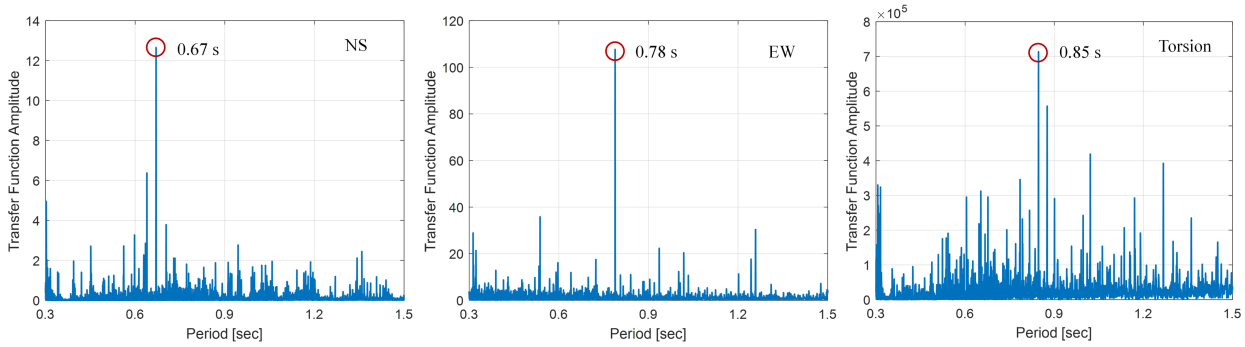


Fig. 11: Building periods identified in the NS, EW, and torsional directions using PEER-CENTS.

## 6. Concluding Remarks and Future Work

This paper documents the implementation of SMA-augmented tension rods to enhance the seismic performance of the GEC at the University of California, Berkeley. The study combined proof-of-concept shaking table testing, component and frame validation tests, nonlinear analysis, building implementation, and field verification. The main conclusions are as follows:

1. Shaking table tests showed stable SMA brace behavior, with no cable failure, no permanent deformation, and no damage or slippage in the tension rod assembly under repeated strong motions.
2. These tests also highlighted the need for a center rod to control out-of-plane motion, which was incorporated into the final building implementation.
3. Full-scale cable and device tests confirmed the importance of pre-training and demonstrated stable superelastic hysteresis, strong recentering capability, and repeatable behavior.
4. Reduced-scale frame tests showed that the SMA-braced frame provided strong self-centering together with appreciable energy dissipation, supporting the expected seismic performance of the system.
5. Field tests using PEER-CENTS and conventional accelerometers identified natural periods that agreed well with the numerical model, supporting model fidelity and the use of PEER-CENTS for SHM.
6. The verified numerical model showed that SMA tension rods reduced floor accelerations by 10%, peak story drifts by 20%, torsional response by 35%, residual drifts by 50% on average and up to 75%, and BRB frame demands, thereby improving post-earthquake resilience and enabling faster reoccupancy.

The GEC also provides an important case for future near-fault response studies. The PEER-LBNL Simulated Ground Motion Database (SGMD) [7] enables the use of non-ergodic, site-specific simulated motions, and future work will evaluate the building response using simulated ground motions from magnitude 7.0 Hayward Fault events at the site. Refer to Fig. 12 for preliminary results with the following key remarks:

- FN and FP denote the fault-normal and fault-parallel components. Station S_20_20 is the SGMD site

closest to the GEC with similar site conditions, $V_{s30}$ = 250 m/s (ASCE Site Class D).

- The ASCE 7-22 Design and MCER spectra for the GEC and S_20_20 sites are broadly similar.
- Over the period range most relevant to the GEC (≈ 0.55 to 0.89 s), the SGMD median and median +$\sigma$ compare reasonably well with the code-based spectra.
- At longer periods, the SGMD spectra fall below the code spectra, suggesting that the code hazard includes stronger long-period contributions.
- Earthquakes with different hypocenters and rupture characteristics on the same fault can produce substantially different ground shaking at the building site, capturing motion-to-motion variability.

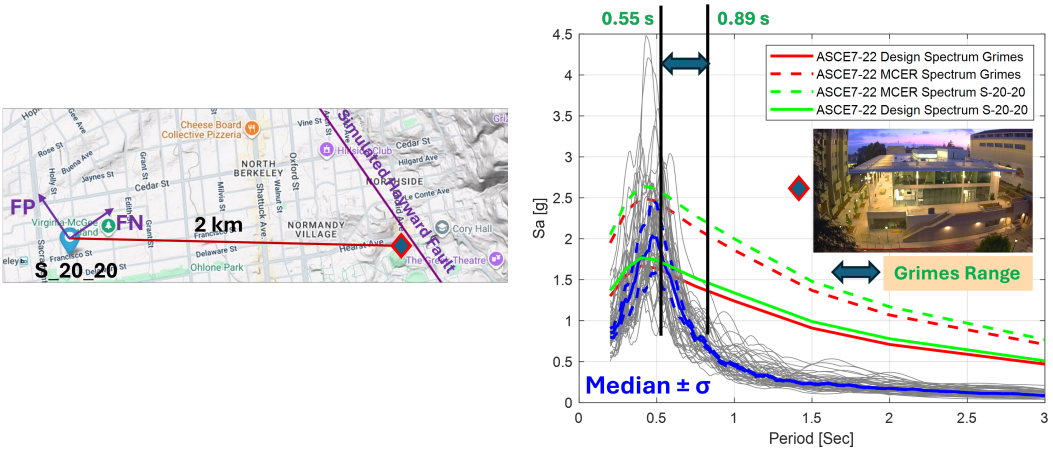


Fig. 12: SGMD station S_20_20 in downtown Berkeley (left), and acceleration response spectra of FN component from 50 realizations (gray plots), together with Design and risk targeted MCER spectra.

## Acknowledgments

Special thanks are due to students and postdocs of the STAIRlab group and staff from PEER Center for their assistance with the field tests using the EMS.

## References

[1] B. Andrawes, *Shape Memory Alloys in Civil Engineering*. Cham, Switzerland: Springer, 2024.

[2] O.E. Ozbulut, S. Hurlebaus, and R. DesRoches, "Seismic response control using shape memory alloys: A review," *Journal of Intelligent Material Systems and Structures*, 22(14):1531–1549, 2011.

[3] W.-S. Chang and Y. Araki, "Use of shape-memory alloys in construction: A critical review," *Proceedings of the Institution of Civil Engineers – Civil Engineering*, 169(CE2):87–95, 2016.

[4] H. Huang, W.-S. Chang, and K.M. Mosalam, "Feasibility of shape memory alloy in a tuneable mass damper to reduce excessive in-service vibration," *Structural Control & Health Monitoring*, 24(2):e1858, 2017.

[5] American Society of Civil Engineers (ASCE), *Seismic Evaluation and Retrofit of Existing Buildings*, ASCE/SEI 41–17, Reston, VA, 2017.

[6] Computers and Structures, Inc., *ETABS: Extended Three-Dimensional Analysis of Building Systems*, Version 22.0.0, Berkeley, CA, USA, 2024.

[7] D.B. McCallen, A. Pitarka, H. Tang, R. Nakata, K.M. Mosalam, F. Petrone, S. Günay, and C.M. Perez, "An open-access simulated earthquake ground-motion database for an M7 Hayward Fault earthquake in the San Francisco Bay Region," *Earthquake Spectra*, 41(3):2560–2597, 2025.